Brazilian Journal
of Chemical
Engineering

ISSN 0104-6632
Printed in Brazil
www.abeq.org.br/bjche

Vol. 32, No. 01, pp. 167 - 177, January - March, 2015
dx.doi.org/10.1590/0104-6632.20150321s00002751

USING A DOE AND EIS TO EVALUATE THE SYNERGISTIC EFFECTS OF LOW TOXICITY INHIBITORS FOR MILD STEEL

G. V. Bueno, M. E. Taqueda, H. G. de Melo and I. C. Guedes*

Chemical Engineering Department, Polytechnic School of the University of Sao Paulo,
PO Box: 61.548, CEP: 05424-970, São Paulo - SP, Brasil.
E-mail: icguedes@usp.br

(Submitted: June 6, 2013 ; Revised: February 14, 2014 ; Accepted: April 5, 2014)

Abstract - Inhibitors are widely used to prevent corrosion in cooling-water systems, and their protective performance can be enhanced by combination. The aim of this paper is to identify possible synergistic effects between four low toxicity substances used as corrosion inhibitors for mild steel in industrial cooling-water systems. Electrochemical measurements were obtained following a design of experiments (DOE) where the independent variables were the inhibitors concentrations and the response variable the charge transfer resistance estimated from impedance diagrams. Potentiodynamic polarization curves show that all of them act as anodic corrosion inhibitors. Among the tested formulations, only the interaction between sodium molybdate and sodium tungstate showed statistically significant effects, indicating that they can perform better when used together. The results of this work show the importance of using a statistical tool when designing inhibitor mixtures.
Keywords: Mild steel (ASTM 1005); Cooling water; Corrosion inhibitors; Design of experiment; Synergic effects.

INTRODUCTION

In industrial cooling-water systems it is common to use corrosion inhibitors in order to prevent metallic corrosion and its unwanted adverse consequences for operating conditions such as blockages or possible leaks. Until the 80s, much of the corrosion inhibitor formulation was based on hexavalent chromium salts (chromates), due to their low cost and excellent performance to protect different metallic substrates in several aqueous environments (Gouda and Sayed, 1973; Hoar and Evans, 1932; Igual *et al.,* 2007; Lemaitre *et al.,* 1989; Mccafferty, 1989; Onuchukwu *et al*., 1984). However, because of their high toxicity, the use of these compounds is being increasingly restricted by environmental regulations. From this point of view – to seek sustainable development – there is a search for substances that exhibit favorable environmental characteristics **(**Kolman and Taylor, 1993; Murilo *et al.,* 2002; Saji and Shibli, 2002; Sastri, 2001; Shibli and Saji, 2005; Shibli and Kumari, 2004; Souza, 2005; Ullmanns, 1992).

Molecules such as sodium molybdate, sodium tungstate, copper phthalocyanine and a modified polydimethyl-siloxane copolymer (CPPM), with molecular weight of 17,000 g mol^{-1}, have been reported to present corrosion inhibiting properties (Kolman and Taylor, 1993; Murilo *et al.,* 2002; Saji and Shibli, 2002; Sastri, 2001; Shibli and Saji, 2005; Shibli and Kumari, 2004; Souza, 2005; Ullmanns, 1992) while having low toxicity levels and bioaccumulation (Diamatino *et al.,* 2000; Mu *et al.,* 2006; Koutsispyros *et al.,* 2006; Souza, 2005; Ullmanns, 1992).

All these features provide conditions for preparing environmentally friendly corrosion inhibitor formulations to protect metallic materials in hostile environments, and, as a result, work in order to minimize negative ecological impacts, especially if

*To whom correspondence should be addressed

the disposal is done in nature (Igual *et al.,* 2007; Murilo *et al.,* 2002; Saji and Shibli, 2002; Sastri, 2001; Shibli and Saji, 2005; Shibli and Kumari, 2004; Souza, 2005; Virtanen *et al.,* 2001).

With the purpose of minimizing costs and increasing the inhibition efficiency, it is common to use mixtures of inhibitors. It has been reported that mixtures of two different types of compounds can behave better than the substances alone (Alexander and Moccari, 1993; Guedes *et al*., 1998; Leite *et al.,* 2005; Mohammedi *et al.,* 2004; Naderi *et al.,* 2009; Okafor *et al.,* 2010; Silva *et al.,* 2006). The synergistic effects have been ascribed to different mechanisms. For instance, Okafor *et al.* (2010) reported that 2-undecyl-1-sodium ethanoate-imidazoline stabilizes the adsorption of thiourea on steel surface, while Mohammedi *et al.* (2004) ascribed the better performance of HEDP (1-hydroxyethylene-1,1-diphosphonic acid) and sodium metasilicate pentahydrate (Na_2SiO_3. $5H_2O$) in the protection against corrosion of carbon steel in industrial hard water to pure additive effects. On the other hand, Ochoa *et al.* (2002) identified a competitive adsorption process in the corrosion protection of carbon steel in chloride-containing solution by phosphonocarboxylic acid salts and fatty amines. However, a literature survey revealed that many of the published works seeking synergistic effects between inhibitors were performed with only two substances and only a few studies were carried out using three inhibitors (Alexander and Moccari, 1993)**.** This is comprehensible because evaluation of the contributions of individual components to the corrosion inhibition process when more than two substances are added together can be difficult, especially regarding the quantification of synergistic effects between them (Guedes *et al*., 1998; Leite *et al.,* 2005; Ochoa *et al.,* 2002).

Factorial design is useful for identifying synergistic effects of one or more variables on a response. This tool is economical and easy to use and is able to provide a great deal of valuable information. Such a statistical tool allows synergistic effects between different parameters to be quantified based on a limited number of planned experiments; quantitative analyses are performed using adequate software. Typical applications of this approach to different research domains can be found in Saji and Shibli (2002) and Samiento-Bustos *et al.* (2008). A comprehensible explanation about the methodology is presented by Box *et al.* (2005).

This work aims to identify synergistic effects between four low-toxicity substances used as corrosion inhibitors for mild steel (ASTM (1005)) in an industrial cooling water environment. With this purpose, the investigation was performed using a full factorial design of experiments (DOE) in order to quantify more accurately the statistically significant effects that may exist between the inhibitors (Box *et al.,* 2005).

EXPERIMENTAL DESIGN

The interactions between the inhibitors were evaluated using a full factorial design of experiments (DOE) at two (n = 2) levels. The input variables were the four different types of inhibitors (k = 4), which were either absent or added to the corrosive medium at a concentration of 1 x 10^{-3} mol L^{-1}, making the two levels of the project. This combination gives a total of 16 (n^k) experiments (Box *et al.,* 2005).

The original levels of the independent variables (inhibitor concentrations) were coded as -1 and +1 (Table 1). As these variables are continuous, a linear relationship must be established between the real value and the coded value, according to Eq. (1):

$$X_i = \frac{R - \overline{R}}{(R_{máx} - R_{mim})/2} \quad (1)$$

where X_i is the codified variable (= 1, 2, .. k); R is any real value between the minimum and the maximum; $\overline{R}$ is the average between the real minimum and maximum; R_{min}, R_{max} are the extreme values in original units.

Table 1: Codified and real values of the independent entry variable.

Codified values of the entryvariable	Real values of the entry variable (concentration) / mol L^{-1}
- 1	0
+ 1	$1.0x10^{-3}$

Using the codified variables, the experimental matrix of the DOE was built. The set of experiments is designed with each input variable assuming either its minimum (-1) or maximum (+1) value, as presented in Table 2. In this table, the first two columns represent, respectively, the number of the experiment in both standard and run order; this latter was determined by random drawing to avoid systematic errors (Box *et al.,* 2005). The next four columns show the whole set of experimental conditions with codified input variables, while the last four present their correspondence with the input variables assuming their real values.

Table 2: Experimental matrix of the DOE with variables in coded and real values.

Order		Codified input variables				Input variables with real value concentration /mol L^{-1}			
Standard	run	Na_2MoO_4	CPPM	Na_2WO_4	Ft-Cu	Na_2MoO_4	CPPM	Na_2WO_4	Ft-Cu
1	12	-1	-1	-1	-1	0	0	0	0
2	9	1	-1	-1	-1	$1.0x10^{-3}$	0	0	0
3	3	-1	1	-1	-1	0	$1.0x10^{-3}$	0	0
4	16	1	1	-1	-1	$1.0x10^{-3}$	$1.0x10^{-3}$	0	0
5	13	-1	-1	1	-1	0	0	$1.0x10^{-3}$	0
6	2	1	-1	1	-1	$1.0x10^{-3}$	0	$1.0x10^{-3}$	0
7	4	-1	1	1	-1	0	$1.0x10^{-3}$	$1.0x10^{-3}$	0
8	8	1	1	1	-1	$1.0x10^{-3}$	$1.0x10^{-3}$	$1.0x10^{-3}$	0
9	6	-1	-1	-1	1	0	0	0	$1.0x10^{-3}$
10	7	1	-1	-1	1	$1.0x10^{-3}$	0	0	$1.0x10^{-3}$
11	1	-1	1	-1	1	0	$1.0x10^{-3}$	0	$1.0x10^{-3}$
12	11	1	1	-1	1	$1.0x10^{-3}$	$1.0x10^{-3}$	0	$1.0x10^{-3}$
13	5	-1	-1	1	1	0	0	$1.0x10^{-3}$	$1.0x10^{-3}$
14	10	1	-1	1	1	$1.0x10^{-3}$	0	$1.0x10^{-3}$	$1.0x10^{-3}$
15	14	-1	1	1	1	0	$1.0x10^{-3}$	$1.0x10^{-3}$	$1.0x10^{-3}$
16	15	1	1	1	1	$1.0x10^{-3}$	$1.0x10^{-3}$	$1.0x10^{-3}$	$1.0x10^{-3}$

EXPERIMENTAL

Samples of mild steel ASTM 1005 with the following chemical composition (wt%): 0.05C; 0.3Mn; 0.05Al; 0.016P; 0.011S; 0.010Cr; 0.002Ni and balance Fe were employed. The specimens were cut into round-shaped working electrodes, mechanically polished with different SiC emery papers (320, 400 and 600 grit), washed with distilled water, rinsed with ethanol and acetone and dried in a hot air stream.

The cooling water used in this investigation was supplied by Oxiteno Company, in São Paulo, Brazil, from its industrial site, and its composition is presented in Table 3. Further analysis revealed pH 6.9 and conductivity of 1100 μS cm^{-1}.

The substances used as corrosion inhibitors were sodium molybdate, sodium tungstate, copper phthalocyanine and a polydimethyl-modified siloxane copolymer (CPPM). When present, they were added to the corrosive medium at a concentration of 1 x 10^{-3} mol L^{-1}.

Electrochemical Techniques

All the electrochemical tests were carried out in naturally aerated solutions (35 cl) at 25±1 ºC using a classical three-electrode cell mounting, employing a large area Pt grid as counter-electrode and $Ag/AgCl_{(KCl\ saturated)}$ as reference electrode. In order to minimize the ohmic drop; this latter was connected to the main cell compartment by means of a Luggin capillary.

The electrochemical techniques employed to evaluate the corrosion inhibition efficiency of the different molecules were electrochemical impedance spectroscopy (EIS) and anodic and cathodic potentiodynamic polarization curves. The EIS spectra were acquired after 3 hours of stabilization of the corrosion potential (E_{corr}) in the frequency range from 10 kHz to 125 mHz and at an acquisition rate of 10 points per decade. The perturbation amplitude was 10 mV (rms). After the completion of the EIS experiments the system was allowed to return to the stationary condition and the anodic and cathodic polarization curves run. The potential range studied varied from - 1600 mV to + 1200 mV versus OCP and the scan rate was 1 mV s^{-1}.

The electrochemical tests were performed using an EG&G Princeton Applied Research (model 273) Potentiostat/Galvanostat coupled to a Solatron 1255 frequency response analyzer. The equipments were coupled to a PC and piloted by the Zview® software.

Table 3: Chemical composition of water from the cooling system used in this study.

Ion	ppm
Ca^{2+}	125
Fe^{2+}	1.20
Si	11.3
Total chloride	3.0
Free chloride	1.0
Cl^-	326
Total hardness (Ca^{2+}, Mg^{2+})	175
Suspended solids	52.5
Alkalinity (KOH)	90.0

RESULTS AND DISCUSSION

Analysis of the Electrochemical Results for Each Inhibitor Added Individually

Figure 1 presents the polarization curves obtained in the presence of $1x10^{-3}$ mol L^{-1} of each inhibitor added individually. The curves were acquired after 3.5 hours of immersion of the electrodes in the test solutions. The addition of each inhibitor to the corrosive medium shifted E_{corr} to more positive values, indicating that all the studied substances behave as anodic corrosion inhibitors. Smaller anodic currents were found in the following order: sodium tungstate ≈ sodium molybdate < polydimethyl-modified siloxane copolymer < copper Phthalocyanine, indicating better performance for the first two inhibitors. For the inhibitors that presented the lowest anodic currents (sodium tungstate and sodium molybdate), a clear passive region was verified, which can be indicative of insoluble film formation between the inhibitors and the ions of the corroding metal (Samiento-Bustos *et al.,* 2008; Shibli and Saji, 2005). In the solution containing molybdate, the substrate exhibited the smallest passive current density, and a repassivation peak was detected at approximately – 400 mV (Ag/AgCl), which can be likely due to the precipitation of a protective film. On the other hand, the largest passive range, *ca* 1000 mV, and the highest pitting potential was observed when tungstate was added to the test solution, pointing towards a more stable passive film. Concerning the cathodic behavior all the inhibitors behave similarly, and presented slightly higher currents when compared to the substrate immersed in the solution without inhibitor.

The analysis of the polarization curves presented in Figure 1 shows that cathodic branches display a typical Tafel behavior, with a log/linear variation of the current with decreasing potential. On the other hand, the anodic branches acquired in the inhibitor-containing solution clearly deviate from the Tafel comportment. Similar anodic response has been observed by other authors in studies on corrosion inhibitor efficiency for steel in different media. They have being associated with the presence of adsorbed species or insoluble corrosion products on the electrode surface.

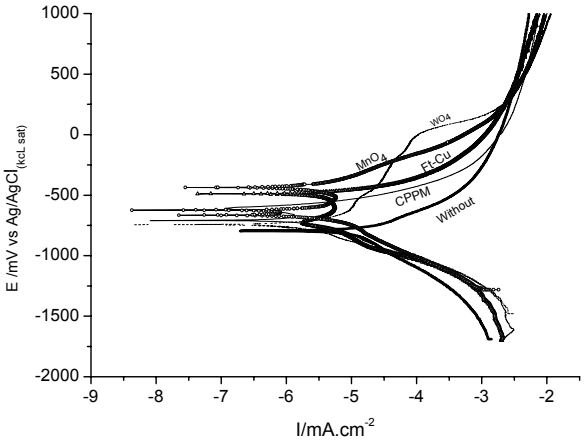

Figure 1: Potentiodynamic polarization curves for mild steel ASTM 1005 in the cooling-water in the absence and in the presence of 1 x 10^{-3} mol L^{-1} of each inhibitor.

Table 4 displays the values of the electrochemical parameters derived from the Tafel extrapolation procedure applied to the polarization curves presented in Figure 1. Due to the reason exposed above, the anodic slope (βa) was not obtained and, therefore, the polarization resistance could not be calculated. Accordingly, icorr values were determined by extrapolation of the cathodic branch to Ecorr. The addition of the inhibitor to the electrolyte shifts Ecorr in the noble direction and decreases the cathodic Tafel slopes, which must be a consequence of the lower anodic current density for the steel when the inhibitors are added to the test electrolyte. The inhibition efficiency calculated using Eq. (2) showed that Na_2WO_4 affords the best corrosion protection, with inhibition close to 86%, whereas Ft-Cu is the least efficient inhibitor, with inhibition efficiency close to 26%.

Table 4: Electrochemical corrosion parameters derived from the Tafel extrapolation method, and calculated inhibition efficiency for the different inhibitors.

	Inhibitors				
Tafel parameters	**0.00**	**Ft-Cu**	**CPPM**	**Na_2MoO_4**	**Na_2WO_4**
βa ($mV.dec^{-1}$)	218				
βc ($mV.dec^{-1}$)	-300	-214	-142	-262	-152
Ecorr (mV)	-800	-660	-667	-680	-757
icorr ($A.cm^{-2}$)	1.2×10^{-5}	8.9×10^{-6}	8.0×10^{-6}	5.3×10^{-6}	1.6×10^{-6}
η (%)	0.00	26	33	56	86

$$\eta(\%) = \frac{i_{corr(0)} - i_{corr(i)}}{i_{corr(0)}} \cdot 100 \quad (2)$$

The EIS diagrams obtained in the presence of each individual inhibitor are presented in Figure 2.

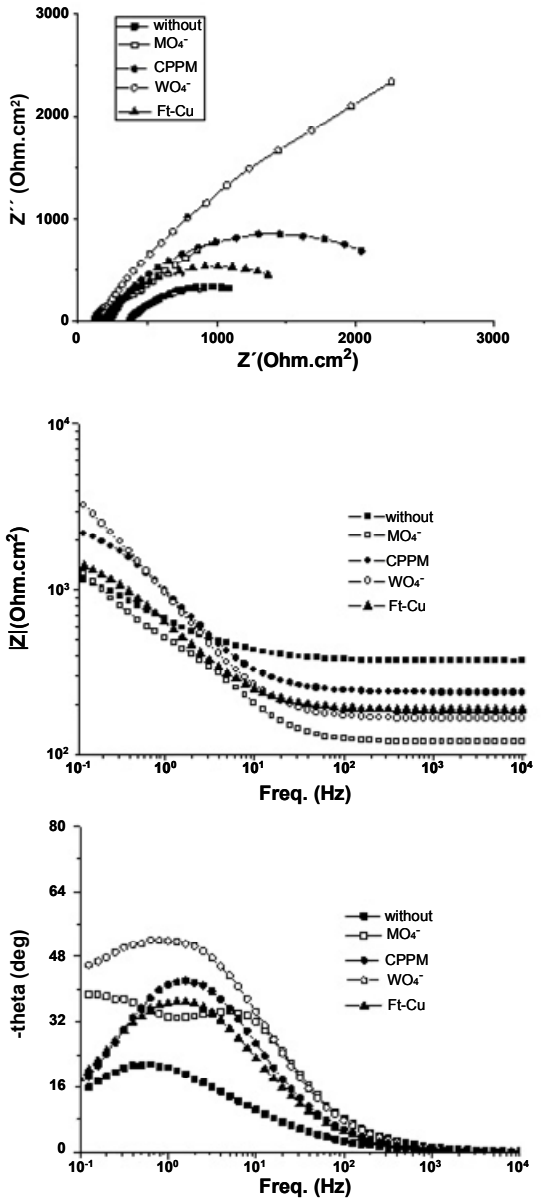

Figure 2: EIS diagrams for mild steel ASTM 1005 in the cooling-water in the absence and in the presence of 1 x 10^{-3} mol L^{-1} of each inhibitor.

Similar to results reported by other authors (Granero *et al*., 2009; Samiento-Bustos *et al.,* 2008), all diagrams exhibit depressed capacitive loops, indicating that complex phenomena are taking place at the interface. In accordance with the polarization curves, the results show that all the substances increase the impedance response, demonstrating that they are hindering the corrosion activity to different extents. Due to the low conductivity of the medium, the electrolyte resistance is rather high, and the addition of the inhibitors causes a clear decrease in this parameter.

Examination of Figure 2 reveals that one and two time constant responses were obtained. As the aim of the present work is not to determine the inhibition mechanism of the different molecules but to identify possible synergistic effects between them using a statistical tool, the origin of the different time constants will not be exhaustively discussed. However, in the literature, one time constant EIS response has been associated with molecules that adsorb onto the metallic substrate, changing the properties of the electrical double layer (Mahdavian and Ashhari, 2010), while two time constants have been ascribed to film forming corrosion inhibitors (Leite *et al.,* 2005; Kalman *et al.,* 1994). Virtanen *et al.* (2001) and Alexander and Moccari (1993) reported evidences of film formation between molybdate ions and iron in different media. These latter authors (Alexander and Moccari, 1993) have proposed that the protective film could be formed either by the reaction of Fe^{2+} ions with MoO_4^{2-} or by the interaction of a coordinated molybdate complex with the unfilled orbital (d) of the steel substrate.

Using the presented reasoning, the high frequency (HF) relaxation phenomena of the diagrams acquired in sodium molybdate and tungstate-containing electrolytes, which show two time constants, can be attributed to the presence of a film formed by the inhibitors with the corrosion products, a hypothesis in accordance with the anodic passive behavior observed when they were added to the test electrolyte. On the other hand, the low frequency (LF) loop can be ascribed to interfacial phenomena, namely, the double layer capacity (C_{dl}) in parallel with the charge transfer resistance (R_{ct}). This latter process is responsible for the single time constant verified in the EIS diagrams of mild steel when the two other inhibitors were added to the corrosive medium.

The EIS diagrams for mild steel in the presence of tungstate and molybdate ions presented in Figure 2 are qualitatively very similar to those obtained by Kolman and Taylor (1993) for pre-corroded mild steel samples in natural waters containing molybdate ions. These authors observed an increase in the HF loop diameter with increasing inhibitor concentration, which they interpreted as being due to charge transfer resistance. However, this interpretation cannot be considered correct since a corrosion product layer was previously present at the sample surface, as stated by the authors. Therefore the HF loop must be likely ascribed to the response of this corrosion

product layer (in another part of the article the authors state "increasing charge transfer resistance may have been the result of increasing concentrations of Na_2MoO_4 that converted the non-protective iron oxide/hydroxide to an increasingly protective ferrous-ferric-$Na_2MoO_4^{2-}$ barrier" additionally supporting our criticism). The correct interpretation of the results of this work (Kolman and Taylor, 1993) further corroborates the hypothesis that the HF capacitive loop verified in the EIS response of mild steel in the presence of these two inhibitors is due to the existence of a corrosion product layer formed between the inhibitors and the ions resulting from the corrosion process. The analysis of the absolute values of the impedance in the LF limit of Figure 2 is in qualitative agreement with the results of the inhibition efficiencies presented in Table 4, and allows the classification of the corrosion inhibition efficiency as follows: modified Ft-Cu < CPPM < sodium molybdate < sodium tungstate.

In order to have a better quantitative evaluation of the effects of the inhibitors on the corrosion behavior of the substrate the EIS responses were fitted using equivalent circuits (EC). Figure 3 presents the two ECs employed to fit either the one (Figure 3(a)) or the two (Figure 3(b)) time constant EIS diagrams. In both ECs, constant phase elements (CPE) were used to replace pure capacitances in order to take into account non-homogeneities of the systems (Gerengi *et al.,* 2009; Jorcin, *et al.,* 2006; Popova and Christov, 2006), which is reflected in the depressed nature of the capacitive loops. The dispersion of the capacitive semicircle is explained either by surface heterogeneities due to surface roughness or impurities, inhibitor adsorption and formation of porous layers. In this sense the CPE exponent, n, can serve as a measure of the surface heterogeneity. In the ECs of Figure 3, R_s, R_p and R_{ct} stand for the solution resistance, the pore resistance of the film and the charge transfer resistance, respectively, while CPE-film represents the capacity of the film formed on the substrate surface in the presence of tungstate and molybdate and CPE-dl the capacity of the electrical double layer, both of them exhibiting frequency distributed properties. Fitting was considered successful when the errors associated with the estimation of each passive element was inferior to 10% and when chi-squared was lower than 10^{-3}.

Table 5 displays the results of the fitting procedure of the diagrams presented in Figure 2 with the ECs of Figure 3. The results of the charge transfer resistance (R_{ct}) calculations are in full agreement with the tendency evaluated by the Tafel extrapolation method. Therefore, the inhibition efficiency can be classified as follow: Na_2WO_4 (93 %) >> Na_2MoO_4 (61 %) > CPPM (49%) > Ft-Cu (24%). These values were superior to those determined from the polarization curves (Table 4), which can be likely ascribed to the better precision of the EC fitting procedure. The analysis of the data presented in this table also indicates that the film formed in the tungstate-containing solution must be very porous. Thus, it exhibits low resistance and the CPE exponent of the LF time constant when this inhibitor is added to the test electrolyte is close to 0.5, indicating the onset of a diffusion controlled process.

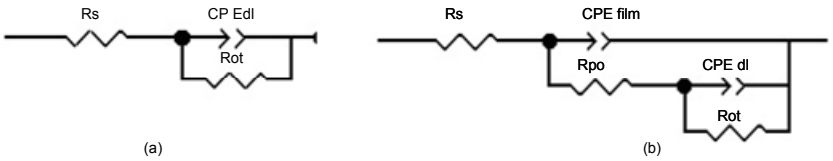

Figure 3: Equivalent circuits used to fit the EIS diagrams obtained in the DOE: (a) one time constant; (b) two time constant diagrams.

Table 5: EC parameters obtained from the fitting of the impedance diagrams presented in Fig. 2 with the equivalent circuits of Figure 3.

	Inhibitors				
Parameters	**0.00**	**Ft-Cu**	**CPPM**	**Na_2MoO_4**	**Na_2WO_4**
R_s ($\Omega.cm^2$)	368	183	236	119	165
CPE-T_{film} ($F.cm^{-2}.s^{(n-1)}$)	-	-	-	0.00020	0.00011
n	-	-	-	0.87	0.91
R_{film} ($\Omega.cm^2$)	-	-	-	419	49
CPE-T ($F.cm^{-2}\ s^{(n-1)}$)	0.00073	0.00042	0.00023	0.00096	0.00024
n	0.63	0.74	0.79	0.74	0.52
R_{ct} ($\Omega.cm^2$)	1207	1592	2360	3088	17047
Chi-squared (10^4)	1.8	2.4	1.7	0.62	0.52
η (%)	0.00	24	49	61	93

Identification of Synergistic Effects Using the DOE

In a DOE, in order to quantify the effects of the input variables, it is necessary to choose a response variable. In the present investigation this was the R_{ct} estimated from the EC fitting of the EIS diagrams. This variable was chosen as it is directly related to the corrosion resistance, *i.e.*, the higher it is the better the corrosion protection afforded by the inhibitors. The values of R_{ct} obtained in the experiments of the DOE are presented in Table 6, wherein the amount of inhibitor is presented in codified variables; moreover, in order to facilitate the statistical analysis, a label "X_i" was associated with each inhibitor.

Table 6: Experimental matrix with the input variables coded (molar concentration of substances) and response variable (R_{ct}) for each experiment proposed in the full factorial design.

Coded input variables					
	X_1	X_2	X_3	X_4	Response variable
Standard	Na_2MoO_4	CPPM	Na_2WO_4	Ft-Cu	R_{ct} ($\Omega.cm^2$)
1	-1	-1	-1	-1	1173
2	1	-1	-1	-1	3773
3	-1	1	-1	-1	2353
4	1	1	-1	-1	5714
5	-1	-1	1	-1	20940
6	1	-1	1	-1	**35673**
7	-1	1	1	-1	13358
8	1	1	1	-1	**35235**
9	-1	-1	-1	1	1584
10	1	-1	-1	1	15311
11	-1	1	-1	1	2365
12	1	1	-1	1	5772
13	-1	-1	1	1	22331
14	1	-1	1	1	**37924**
15	-1	1	1	1	10439
16	1	1	1	1	27548

The results show that any combination of inhibitor hinders the corrosion process to some extent (the lowest R_{ct} was verified when no inhibitor was added to the solution – experiment 1). A preliminary analysis of the data also demonstrates that the best inhibitory efficiencies were obtained in experiments 6, 8 and 14. In all of them, the concentrations of Na_2MoO_4 and Na_2WO_4 were at their maxima; however, the concentration of CCPM and Ft-Cu were either at their maxima or minima. The results presented in the table also show that the estimated values of R_{ct} for these three experiments are very close; therefore, the prediction of the existence of synergistic effects between the four inhibitors can only be accomplished on the basis of a statistical analysis based on a set of planned experiments as performed in the DOE.

Statistical analysis of the DOE was performed with the Minitab software, and the full result is presented in Table 7. In the overall analysis only individual effects and first-order interactions between each two input variables were considered. In this table the constant term represents an average of all R_{ct} values, obtained with the software, from all the experimental data. Therefore, for all the analyzed variables, the sign associated with each effect indicates if it contributes to increase (+) or decrease (-) this constant term. As already stated, in Table 6, the lowest value of R_{ct} was obtained when no inhibitor was added to the corrosive medium (first experiment in the standard order). Therefore, a negative sign associated with any of the effects only indicates that it contributes to diminish the constant term presented in Table 7, and cannot be straightforwardly associated with acceleration of the corrosion process; conversely, a positive value means that the analyzed effect contributes to increase the average R_{ct}.

Table 7: Results of statistical analysis using Minitab software, which shows the values of the individual effects and interactions of input variables in the R_{ct}. variable.

Variable	Effect	Coef.	SE Coef.	T	p – value
Constant term	16968	16968	1847	9.19	0.000
Na_2MoO_4 **(X_1)**	15301	7650	1847	4,14	0.009
CPPM **(X_2)**	-8241	-4120	1847	-2.23	0.076
Na_2WO_4 **(X_3)**	24425	12213	1847	6.61	0.001
Ft-Cu **(X_4)**	-3118	-1559	1847	-0.84	0.437
X_1*X_2	-3862	-1931	1847	-1.05	0.344
X_1*X_3	9527	4764	1847	2.58	0.050
X_1*X_4	-2842	14.21	1847	-0.77	0.477
X_2*X_3	-6831	-3416	18471	-1.85	0.124
X_2*X_4	484	242	1847	0.13	0.901
X_3*X_4	-6123	-3061	1847	-1.66	0.158

In the DOE the most important variable in order to determine the statistical relevance of each analyzed effect is the significance level associated with it. This was evaluated by the p-value approach, represented in the last column of Table 7, which gives the smallest level of significance that would lead to rejection of the null hypothesis H_o [Box, *et al.* (2005)]. The coefficient is considered significant if it lies below a given threshold. In the present study all the variables with significance level (p-value) below 0.1 (p-value < 0.1) was taken as significant. Using this criterion the only statistically significant effects were: X_1 (Na_2MoO4), X_2 (CPPM), X_3 (Na_2WO_4) and the interaction between X_1 and X_3. Taking into account what was said, Table 8 presents the ANOVA for R_{ct}, considering the three and four factor interactions as degrees of freedom for error estimation.

Table 8: Analysis of variance for significance of the regression model for the Rct variable.

Source	D. F.	Seq SS	Adj SS	Adj Ms	F	P
Main Effects	4	3633385294	3633385294	908346324	16.64	0.004
Interactions	6	792607858	792607858	132101310	2.42	0.175
Residual Error	5	273007911	2730079110	54601582		
Total	15	4699001063				

$R^2 = 82.6\%$ S = 7389.29

In Figure 4 the main effects and interactions are plotted on a probability scale for the 90% confidence interval. In this graph, the farther the point lies from the full line the more statistically significant the effect (Box *et al.,* 2005). In this plot, it is clearly demonstrated that the main statistically significant effects are associated with X_1, X_2, X_3 and the two-factor interaction between X_1 and X_3.

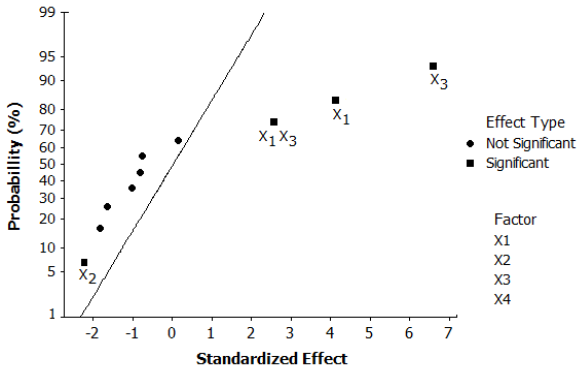

Figure 4: Normal probability plot for the effects of input variables for each substance studied as a corrosion inhibitor.

From the data analysis, the statistical model obtained in order to estimate the R_{ct} value (response variable) as a function of the statistically significant input variables is represented by Eq. (3). It shows that the input variables X_1 (Na_2MoO4) and X_3 (Na_2WO_4) provoked a positive effect in the average R_{ct} value. A positive synergistic effect between these two inhibitors was also observed, indicating that when used together the overall inhibitory effect must be superior to their simple additive effect. On the other hand, the input variable X_2 (CPPM) causes a negative effect in the average value of R_{ct} (note that the negative sign does not mean that the input variable accelerates the corrosion process). Consequently, its addition together with X_1 and X_3 must provoke a decrease in the R_{ct} average value, indicating that somehow it hinders the joint inhibitive action of these two substances. Moreover, the substance with the best individual effect was tungstate (X_3), in accordance with the first part of this manuscript, when the individual effect of each inhibitor was evaluated.

$$R_{ct} = 16968 + 7650X_1 - 4120X_2 + 12213X_3 + 4764X_1X_3 \quad (3)$$

In Figure 5 the plot of the residuals (errors) vs. the estimated values of the response variable (R_{ct}), calculated using Eq. (3), is presented. A random distribution of the residues is observed, suggesting that the model is indeed appropriate.

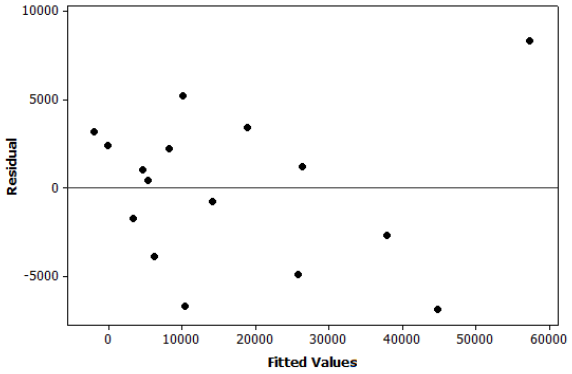

Figure 5: Residual vs. fitted values of the response variable (R_{ct}).

The statistical model presented in Eq. (3) indicates that the addition of the inhibitor Ft-Cu does not provoke any statistically significant effect on corrosion attenuation. This could already be deduced from Figures 1 and 2 where only marginal effects were observed both in the polarization curves and in the EIS diagrams upon addition of this particular inhibitor. But, more important, Eq. (3) also indicates that the addition of this inhibitor does not cause any statistically significant effect on the results of the other combined variables. This would not be easy to conclude simply from the analysis of a set of experiments where different variables were analyzed together.

The contribution of the inhibitor CPPM (X_2) in Eq. (3) shows that it hinders the joint action of molybdate (X_1) and tungstate (X_3). This can be understood if we analyze the inhibition mechanism previously proposed for the different inhibitors based on the EIS results presented in Figure 2. The adsorption of CPPM on the electrode surface can diminish the dissolution of iron and, in consequence, avoid the formation of the corrosion product layer responsible for the corrosion protection afforded by WO_4^{2-} and MoO_4^{2-}. Finally, the synergistic effect detected between these latter two inhibitors can be ascribed to the formation of a more stable protective film. It can be proposed that, as both inhibitors are weak oxidizers **(**Alexander and Moccari, 1993; Kolman and Taylor, 1993; Li *et al.,* 2009; Qu *et. al.,* 2008), it is likely that their mutual oxidizing action will boost the performance of each of them. Indeed, in the literature, it has been reported that the addition of other oxidizing agents like nitrites or oxygen to aggressive solutions containing molybdate improves the corrosion protection afforded by this anion (Alexander and Moccari, 1993).

Figure 6 shows selected EIS diagrams considered relevant for understanding the quantitative analysis presented in Eq. (3). The visual analysis of the diagrams clearly shows that the best protection was afforded by mixing Na_2MoO_4 and Na_2WO_4 or Na_2MoO_4, Na_2WO_4 and CPPM, and that the impedance responses for these combinations were similar. However, the statistical analysis, for which the quantitative evaluation is expressed by Eq. (3), indicated that the addition of CPPM to the mixture of Na_2MoO_4 + Na_2WO_4 provokes a decrease of the joint effect of these two inhibitors, which is apparently contradictory. Nevertheless, one must bear in mind that the statistical analysis is based on the results of a set of experiments and the effects of all of them in all the situations are being evaluated. Table 4 shows that when CPPM is added to a Na_2WO_4-containing solution, there is a decrease in R_{ct} (compare the R_{ct} values for experiments 5 and 7). Moreover, comparing the R_{ct} values for experiments 6, 8 and 14 (those with the best results), those of assays 6 and 14, where CPPM was absent, were slightly superior. In addition, the R_{ct} value for experiment 16 (all inhibitors at their maxima) is considerably lower. Taking into account that, from the statistical point of view, the addition of Ft-Cu is non-significant for the anticorrosion performance of the formulations, in the overall analysis it is considered that these differences are due to the addition of CPPM to a solution containing Na_2MoO_4 + Na_2WO_4, explaining the results expressed in Eq. (3).

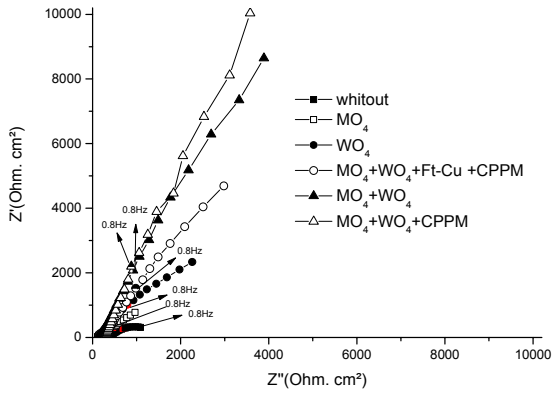

Figure 6: Selected Nyquist diagrams for ASTM 1005 mild steel in the cooling-water used in the plant of Oxiteno – São Paulo (Brazil).

Figure 7 displays the comparison between the polarization curves for the best formulation identified in the DOE analysis (molybdate + tungstate) and those acquired in solutions containing only molybdate or tungstate. They clearly demonstrate the beneficial effect of adding both inhibitors to the aggressive medium: the passive current is diminished, the pitting potential is raised and a clear diffusion-controlled process is detected in the cathodic branch of the diagram indicating that a more resistive film is formed on the electrode surface.

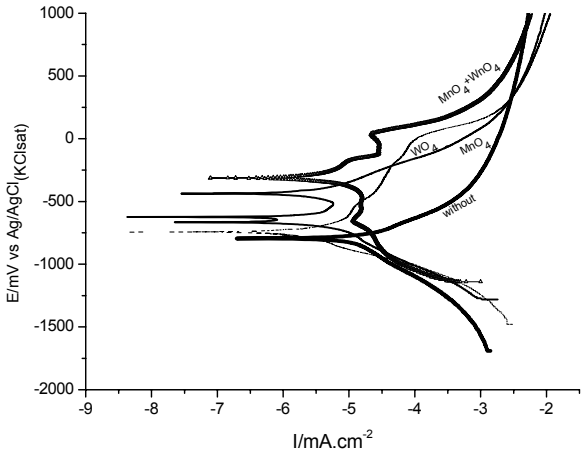

Figure 7: Potentiodynamic polarization curves for mild steel ASTM 1005 in the cooling-water in absence and the presence of different inhibitors: without; MoO_4; WO_4 and MoO_4 + WO_4.

CONCLUSIONS

In the present work a DOE was employed in order to allow the use of statistical tools to quantitatively evaluate synergistic effects between four inhibitors

used to hinder corrosion of mild steel (ASTM 1005) in industrial cooling water. The overall electrochemical results show that, to a greater or lesser extent, each inhibitor alone can hinder steel corrosion, and all of them act as anodic corrosion inhibitors. However, the statistical analysis revealed only the existence of positive synergism between sodium molybdate and sodium tungstate. Therefore, the use of these inhibitors together enhances their individual efficiencies. Moreover, it was also detected that the addition of CCPM to the mixture molybdate + tungstate is detrimental to the joint action of these inhibitors and that, from the statistical point of view, the presence of Ft-Cu is insignificant for the corrosion reduction of ASTM 1005 in the studied medium.

The results of this work have shown the importance of using a statistical tool when designing inhibitor mixtures.

REFERENCES

Alexander, D. B. and Moccari, A. A., Evaluation of corrosion inhibitors for component cooling water systems. Corrosion, 49(11), 921-928 (1993).

Box, G. E. P., Hunter, J. F. and Hunter W. G., Statistics for Experimenters. 2nd Ed. John Willey, New Jersey (2005).

Diamantino, T. C., Guilhermino, L., Almeida, E. and Soares, A. M., Toxicity of sodium molybdate and sodium dichromate to *daphnia magna* straus evaluated in acute, chronic, and acetylcholinesterase inhibition tests. Ecotoxicology and Environmental Safety, 45(3), 253-259 (2000).

Gerengi, H., Darowicki, K., Bereket, G. and Slepski, P., Evaluation of corrosion inhibition of brass-118 in artificial seawater by benzotriazole using Dynamic EIS. Corrosion Science, 51(11), 2573-2579 (2009).

Gouda, V. K. and Sayed, S. M. A., Corrosion behavior of steel in solutions containing mixed inhibitive and aggressive ions. Corrosion Science, 13(11), 841-852 (1973).

Granero, M. F. L., Matai, P. H. L. S., Aoki, I. V. and Guedes, I. C., Dodigen 213-N as corrosion inhibitor for ASTM 1010 mild steel in 10% HCl. Journal of Applied Electrochemistry, 39(8), 1199-1205 (2009).

Guedes, I. C., Aoki, I. V. and Taqueda, M. E. S., Polarisation curves and experiment design as tools in the search of optimised inhibitors mixture formulation for HSLA steel in hydrochloric acid. In: Materials Science Forum, 289, 1237-1244 (1998).

Hoar, T. P., and Evans, U. R., 366. The passivity of metals. Part VII. The specific function of chromates. J. Chem. Soc., 2476-2481 (1932).

Igual Muñoz, A., García Antón, J., Guiñón, J. L. and Pérez Herranz, V., Inhibition effect of chromate on the passivation and pitting corrosion of a duplex stainless steel in LiBr solutions using electrochemical techniques. Corrosion Science, 49(8), 3200-3225 (2007).

Jorcin, J. B., Orazem, M. E., Pébère, N. and Tribollet, B., CPE analysis by local electrochemical impedance spectroscopy. Electrochimica Acta, 51(8), 1473-1479 (2006).

Kalman, E., Varhegyi, B., Bako, I., Felhősi, I., Karman, F. H. and Shaban, A., Corrosion inhibition by 1-hydroxy-ethane-1,1-diphosphonic acid an electrochemical impedance spectroscopy study. Journal of the Electrochemical Society, 141(12), 3357-3360 (1994).

Kolman, D. G. and Taylor, S. R., Sodium molybdate as a corrosion inhibitor of mild steel in natural waters part 2: Molybdate concentration effects. Corrosion, 49(8), 635-643 (1993).

Koutsospyros, A., Braida, W., Christodoulatos, C., Dermatas, D. and Strigul, N., A review of tungsten: From environmental obscurity to scrutiny. Journal of Hazardous Materials, 136(1), 1-19 (2006).

Leite, A. O., Araújo, W. S., Margarit, I. C., Correia, A. N. & Lima-Neto, P. D., Evaluation of the anticorrosive properties of environmental friendly inorganic corrosion inhibitors pigments. J. Braz. Chem. Soc. 16(4), 756- 762 (2005).

Lemaitre, C., Baroux, B., Béranger, G., Chromate as a pitting corrosion inhibitor: Stochastic study. Ok Werkstoffe und Corrosion, 40, 229-236 (1989).

Mahdavian, M., Ashhari, S., Corrosion inhibition performance of 2-mercaptobenzimidazole and 2-mercaptobenzoxazole compounds for protection of mild steel in hydrochloric acid solution. Electrochimica Acta, 55(5), 1720-1724 (2010).

Marin-Cruz, J., Cabrera-Sierra, R., Pech-Canul, M. A., Gonzalez, I., EIS study on corrosion and scale processes and their inhibition in cooling system media. Electrochimica Acta, 51(8), 1847-1854 (2006).

McCafferty, E., Thermodynamic aspects of the crevice corrosion of iron in chromate/chloride solutions. Corrosion Science, 29(4), 391-401 (1989).

Mohammedi, D., Benmoussa, A., Fiaud, C., Sutter, E. M. M., Synergistic or additive corrosion inhibition of mild steel by a mixture of HEDP and metasilicate at pH 7 and 11. Materials and Corrosion, 55(11), 837-844 (2004).

Mu, G., Li, X., Qu, Q. and Zhou, J. Molybdate and tungstate as corrosion inhibitors for cold rolling steel in hydrochloric acid solution. Corrosion Science, 48(2), 445-459 (2006).

Murillo, F. R., Sanchez, R. T., Alonso, A. A., Improving the corrosion resistance of a cooling water system at an ammonium sulfate crystallization plant by corrosion inhibitors. Materials and Corrosion, 53(11), 820-826 (2002).

Naderi, R., Mahdavian, M. and Attar, M. M., Electrochemical behavior of organic and inorganic complexes of Zn (II) as corrosion inhibitors for mild steel: Solution phase study. Electrochimica Acta, 54(27), 6892-6895 (2009).

Ochoa, N., Baril, G., Moran, F. and Pébère, N., Study of the properties of a multi-component inhibitor used for water treatment in cooling circuits. Journal of Applied Electrochemistry, 32(5), 497-504 (2002).

Okafor, P. C., Liu, C. B., Liu, X., Zheng, Y. G., Wang, F. and Liu, C. Y., Corrosion inhibition and adsorption behavior of imidazoline salt on N80 carbon steel in CO2-saturated solutions and its synergism with thiourea. Journal of Solid State Electrochemistry, 14(8), 1367-1376 (2010).

Onuchukwu, A. I. and Lori, J. A., The mechanism of the corrosion inhibition of carbon steel in neutral medium by chromate and nickel ions. Corrosion Science, 24(10), 833-841 (1984).

Popova, A. and Christov, M., Evaluation of impedance measurements on mild steel corrosion in acid media in the presence of heterocyclic compounds. Corrosion Science, 48(10), 3208-3221 (2006).

Qu, Q., Li, L., Bai, W., Jiang, S. and Ding, Z., Sodium tungstate as a corrosion inhibitor of cold rolled steel in peracetic acid solution. Corrosion Science, 51(10), 2423-2428 (2009).

Qu, Q., Li, L., Jiang, S., Bai, W., Ding, Z., Effect of sodium molybdate on the corrosion behavior of cold rolled steel in peracetic acid solution. Journal of Applied Electrochemistry, 39(5), 569-576 (2009).

Saji, V. S. and Shibli, S. M. A., Synergistic inhibition of carbon steel corrosion by sodium tungstate and sodium silicate in neutral aqueous media. Anti-Corrosion Methods and Materials, 49(6), 433-443 (2002).

Samiento-Bustos, E., Rodriguez, J. G., Uruchurtu, J., Dominguez-Patiño, G. and Salinas-Bravo, V. M., Effect of inorganic inhibitors on the corrosion behavior of 1018 carbon steel in the LiBr+ ethylene glycol+ H_2O mixture. Corrosion Science, 50(8), 2296-2303 (2008).

Saremi, M., Dehghanian, C. and Sabet, M. M., The effect of molybdate concentration and hydrodynamic effect on mild steel corrosion inhibition in simulated cooling water. Corrosion Science, 48 (6), 1404-1412 (2006).

Sastri, V. S., Corrosion Inhibitors, Principles and Applications. New York, John Wiley and Sons Ltd. (2001).

Shibli, S. M. A. and Kumary, V. A., Inhibitive effect of calcium gluconate and sodium molybdate on carbon steel. Anti-Corrosion Methods and Materials, 51(4), 277-281 (2004).

Shibli, S. M. A. and Saji, V. S., Co-inhibition characteristics of sodium tungstate with potassium iodate on mild steel corrosion. Corrosion Science, 47(9), 2213-2224 (2005).

Silva, D. K. D., Ribas, G. C., Cunha, M. T. D., Agostinho, S. M. and Rodrigues, P. R., Benzotriazole and tolytriazole as corrosion inhibitors of carbon steel 1008 in sulfuric acid. Portugaliae Electrochimica Acta, 24(3), 323-335 (2006).

Souza, P. R., Comportamento de três moléculas do tipo organo-silano como inibidores de corrosão para o aço ABNT 1005 em meio de HCl 2M. M.Sc. Dissertation, EPUSP. São Paulo-SP (2005). (In Portuguese).

Therdthianwong, A., Manomayidthikarn, P. and Therdthianwong, S., Investigation of membrane electrode assembly (MEA) hot-pressing parameters for proton exchange membrane fuel cell. Energy, 32(12), 2401-2411 (2007).

Ullmanns´s Encyclopedia of Industrial Chemistry. VCH Publishers Inc, 213 (1992).

Virtanen, S., Surber, B. and Nylund, P., Influence of MoO_4^{2-} anion in the electrolyte on passivity breakdown of iron. Corrosion Science, 43(6), 1165-1177 (2001).

Vukasovich, M. S. and Farr, J. P. G., Molybdate in corrosion inhibition – a review. Polyhedron, 5(1), 551-559 (1996).